Comparison of Field Observation with WaterTank Experiment on Air Pollution Concentration in Katmandu Valley

A. Kondo[1], A. Kaga[1], Y. Inoue[1],
M. L. Shrestha[1] & B. Sapkota[2]
[1]*Department of Environmental Engineering, Osaka University, Japan.*
[2]*Tribhuvan University, Nepal.*

Abstract

The air pollution concentration in the winter season of Katmandu valley is very high compared with summer season, because the air pollution concentration was strongly influenced by the inversion layer that is formed at Katmandu valley. This mechanism was simulated by a water tank experiment and by numerical calculation. Thermal stratification was made at the start of the experiment, and the temperature on the bottom of water tank was changed with the period of 12 minute. The updraft wind on the slope and Bénard convection occurred while the bottom temperature was maintained in high temperature. The downdraft wind on the slope occurred and the inversion layer was formed while the bottom temperature was maintained in low temperature. The calculated pollution concentration was qualitatively agreed with the field observation in Katmandu valley.

1 Introduction

The atmospheric pollution in Katmandu, which is the capital of Nepal, is getting worse. The measurement in Meteorological Department shows that TSP concentration in winter season is higher than TSP concentration in summer season. The authors measured the concentration of NO_x and TSP and temperature in Katmandu for two weeks (February 2001). It was found that the concentration of NO_x and TSP became high in the morning and the strong stable layer was formed from the midnight to the early morn-

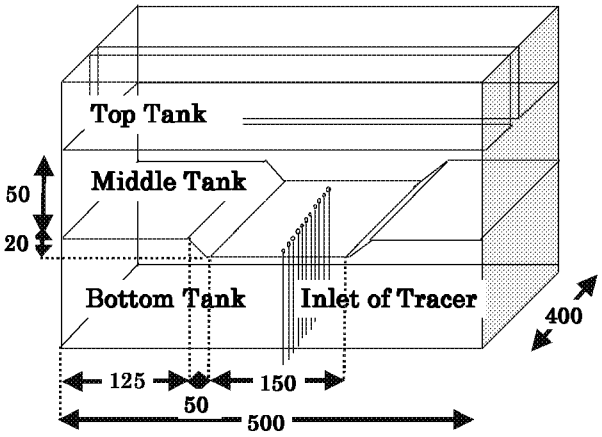

Figure 1: Equipment of water tank experiment

ing [1]. The high atmospheric pollution concentration in the morning is strongly influenced by the stable layer as well as the increase of the traffic volume in the morning. In this paper, we performed the water tank experiment [2] [3] and the numerical experiment for the atmospheric pollution in Katmandu valley and analyzed the mechanism of the high atmospheric pollutant concentration in the morning.

2 Water tank experiment

2.1 Experimetal equipment

The equipment of the water tank experiment is shown in Fig.1. This equipment has three water tanks. The middle water tank (40cm $\times$ 50cm (horizontal) $\times$ 7cm(vertical)) corresponds to the atmosphere of Katmandu valley. The water temperature in the top water tank is kept a constant temperature during experiment in order to keep the water temperature of the upper part of the middle water tank (correspond to the upper atmosphere in Katmandu valley) a constant temperature. The water temperature in the bottom water tank changes with a constant period and a constant amplitude in order to change the lower surface temperature of the middle water tank (correspond to the ground surface in Katmandu valley).

2.2 Experimetal method

The water temperature of the top water tank is kept 40 degree. Simultaneously the water temperature of the bottom water tank is kept 35 degree. After a few hours, the thermal stratification with a constant thermal gra-

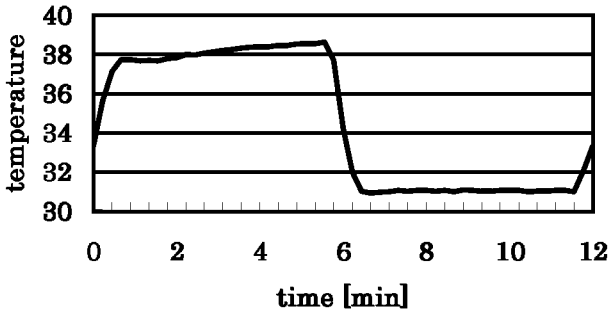

Figure 2: Variation of bottom temperature in the middle water tank

dient is formed in the middle water tank. After that, the lower surface temperature of the middle water tank is changed with the period of 12min as shown in Fig.2. The measurement of the flow field and the concentration is carried out for the third period.

2.2.1 Measurement of temperature

The temperature of the bottom, 5, 10, 15, 20, 40 and 60mm height in the middle water tank was measured by thermo couples. The height of 20mm just corresponds to the mountain height of Katmandu valley.

2.2.2 Measurement of flow field

After the thermal stratification was formed, tracers (MCI GFL High Porous Polymer, 70∼75 μ) were homogeneously injected into the middle water tank. The flow in the middle water tank was visualized by tracers, and video images were taken. The wind vectors were calculated from the movement of tracer patterns between the visualized images [4].

2.2.3 Measurement of concentration

At one minutes before changing the bottom temperature from low temperature to high temperature, tracers (Fluorescein Sodium) instead of pollutant substance were injected from the inlet of the bottom surface of the middle water tank. The decrease of tracers concentration was visualized, and video images were taken.

2.3 Similarity low

Ueda [5] proposed new dimensionless variables that may be the universal similarity variables for comparing field - observation results.

$$U^+ = U^* G_r^{1/2} P_r^{2/3} \tag{1}$$

$$X^+ = X^* G_r^{-0.387} \tag{2}$$

$$Z^+ = Z^* P_r^{1/4} \tag{3}$$

Table 1: Typical values of physical variables in the experiment and in the field

	β [K^{-1}]	ν [m^2/s]	α [m^2/s]
Experiment	0.000207	10^{-6}	1.43×10^{-7}
Field	0.00341	10	10
	ω [rad/s]	Γ [K/m]	$\Delta\Theta$ [K]
Experiment	0.00873	100	7
Field	7.27×10^{-5}	0.005	15

Table 2: Relations between the experiment and the field

	Experiment		Field
Horizontal length	1[mm]	$\rightarrow$	90[m]
Vertical length	1[mm]	$\rightarrow$	56[m]
wind speed	1[mm/s]	$\rightarrow$	4.4[m/s]

where U^* is the dimensionless wind speed, and X^* and Z^* are the dimensionless length of the horizontal direction and the vertical direction, respectively. G_r and P_r are Grashof number and Prandtl number, respectively. The representative wind speed and the representative length are defined by

$$U = g\beta\Delta\Theta/\omega \tag{4}$$

$$L = (\nu/\omega)^{1/2} \tag{5}$$

where g is the gravitational acceleration, β is the volumetric expansion coefficient, $\Delta\Theta$ is the maximum temperature difference of the surface temperature variation, ω is the angular velocity of the earth's rotation and ν is the eddy diffusivity of momentum. Grashof number G_r and Prandtl number P_r are expressed by

$$G_r = g\beta\Gamma L^4/\nu^2 \tag{6}$$

$$P_r = \nu/\alpha \tag{7}$$

where Γ is the mean atmospheric temperature gradient. α is the eddy diffusivity of heat.
The typical values of β, α and etc. in this experiment and in the field are shown in Table 1. The relations of the horizontal length, the vertical length and the wind speed between this experiment and the field can be obtained by using the values of Table 1 and are shown in Table 2. From the relations, the valley depth (2cm) of this experiment corresponds to 1000m depth of the actual Katmandu valley.

3 Numerical model of water tank experiment

3.1 Basic equation

The flow in the middle water tank is assumed to be 2 dimensional laminar flow. Using the Boussinesq approximation, we obtain the following set of the basic equations for the water tank experiment;

$$\frac{du}{dt} = -\frac{1}{\rho}\frac{\partial p'}{\partial x} + \nu\left(\frac{\partial^2 u}{\partial x^2} + \frac{\partial^2 u}{\partial z^2}\right) \tag{8}$$

$$\frac{dw}{dt} = -\frac{1}{\rho}\frac{\partial p'}{\partial z} + \beta T' g + \nu\left(\frac{\partial^2 w}{\partial x^2} + \frac{\partial^2 w}{\partial z^2}\right) \tag{9}$$

$$\frac{\partial u}{\partial x} + \frac{\partial w}{\partial z} = 0 \tag{10}$$

$$\frac{dT}{dt} = \alpha\left(\frac{\partial^2 T}{\partial x^2} + \frac{\partial^2 T}{\partial z^2}\right) \tag{11}$$

where u, w, T and p are the wind speed of the horizontal direction, the wind speed of the vertical direction, temperature and pressure, respectively. The prime is the deviation from the initial value. ρ, ν and α are the density, viscosity coefficient and heat transfer coefficient of water, respectively and are approximated by

$$\rho[\mathrm{g/cm^3}] = -0.5 \times 10^{-5} T_c^2 + 1.0002 \tag{12}$$

$$\nu[\mathrm{cm^2/s}] = 0.046 \times 10^{-4} T_c^2 - 0.438 \times 10^{-3} T_c + 1.703 \times 10^{-2} \tag{13}$$

$$\alpha[\mathrm{cm^2/s}] = -0.003 \times 10^{-5} T_c^2 - 0.062 \times 10^{-4} T_c + 1.31 \times 10^{-3} \tag{14}$$

$$T_c = T - 273$$

3.2 Calculation condition

The calculated region is the same as the x-z section of the experimental equipment and is divided into 181× 40 meshes. The boundary conditions are also the same as the experimental conditions. The basic equations (equation(8) ∼ (11)) were solved by SIMPLE method [6].

4 Comparison of field observation, water tank experiment and calculated results

4.1 Temperature

The temperature variations at 5, 10, 15, 20, 40 and 60mm height obtained from the experiment and from the calculation are shown in Fig.3. The temperature variations occur until 20mm height but do not occur above 20mm height. The temperature increases by Bénard convection while the bottom temperature is maintained by high temperature. The temperature decreases by the cold flow from the top of the mountain (valley wind) while

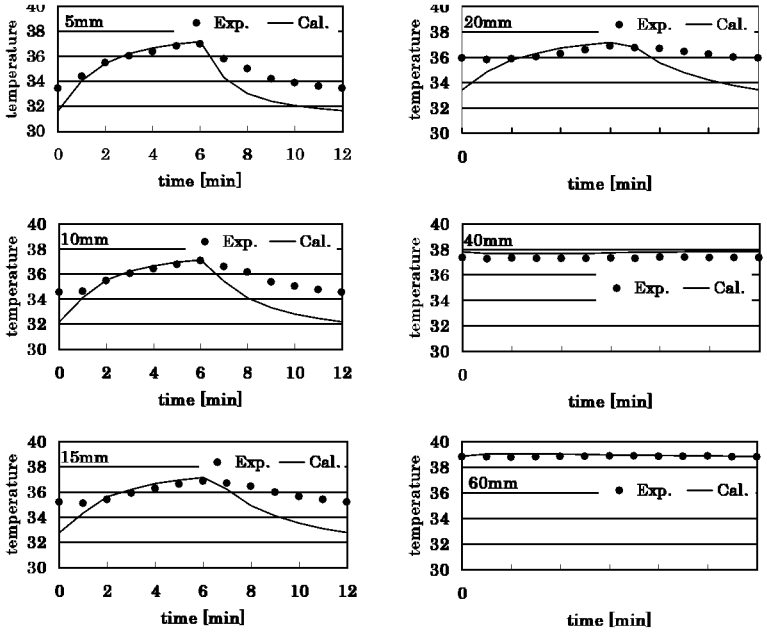

Figure 3: Temperature variations obtained from experiment and from calculation at 5, 10,15,20, 40 and 60mm height

the bottom temperature is maintained by low temperature. The inversion layer is formed. The temperature decrease of the experiment is smaller than that of the calculation, since the calculated valley wind is stronger than the experiment as will be shown later (flow visualized by tracers).

4.2 Flow field

The calculated flow fields of the left side after 1, 3, 5, 7, 9 and 11 minute are shown in Fig.4. The time displayed in Fig.4 corresponds to the period of Fig.2. The updraft wind on the slope (mountain wind) and Bénard convection occur soon after the bottom temperature increases. After that, these flows are getting weaker, but are held, while the bottom temperature is maintained by high temperature. The downdraft wind on the slope (valley wind) occurs soon after the bottom temperature decreases. The counter flow occurs above the valley. After that, the depth of the valley wind is getting thinner.
The flow fields extracyed from video images after 0, 2, 4, 6, 8 and 10minute are shown in Fig.5. These flow fields are generally the same as the calculated flow field.

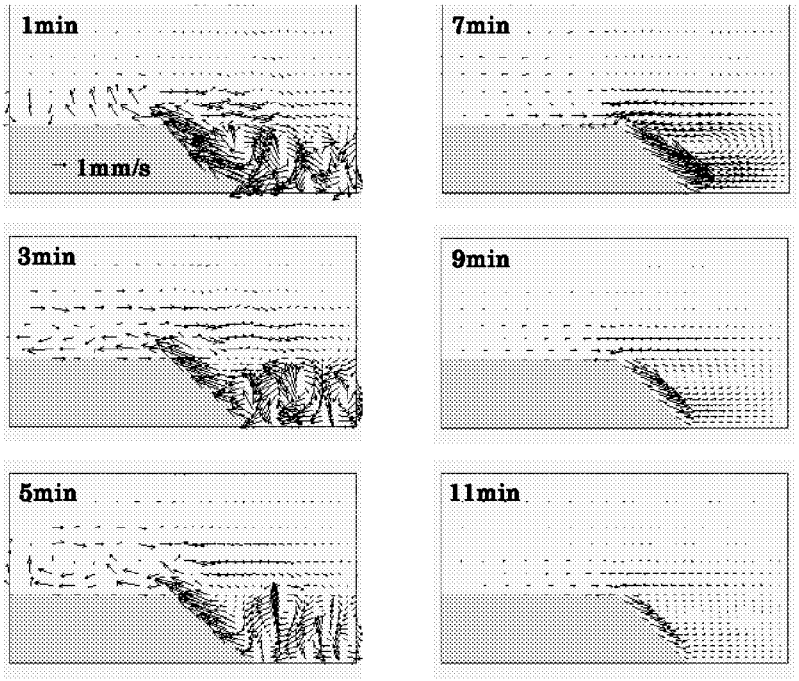

Figure 4: Calculated flow fields after 1, 3, 5, 7, 9 and 11min

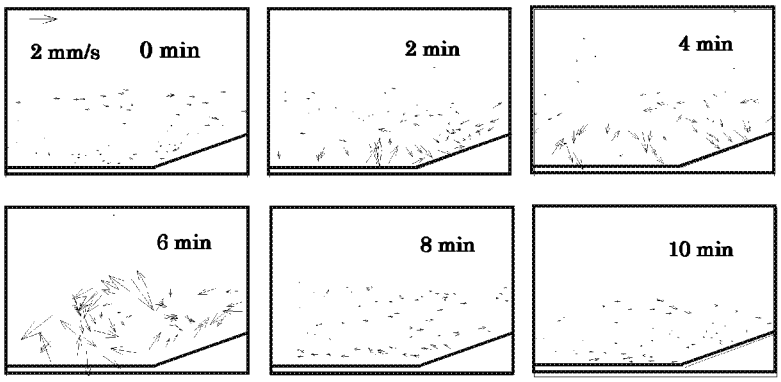

Figure 5: Flow fields extracted from video images after 0, 2, 4, 6, 8 and 10min

4.3 Concentration

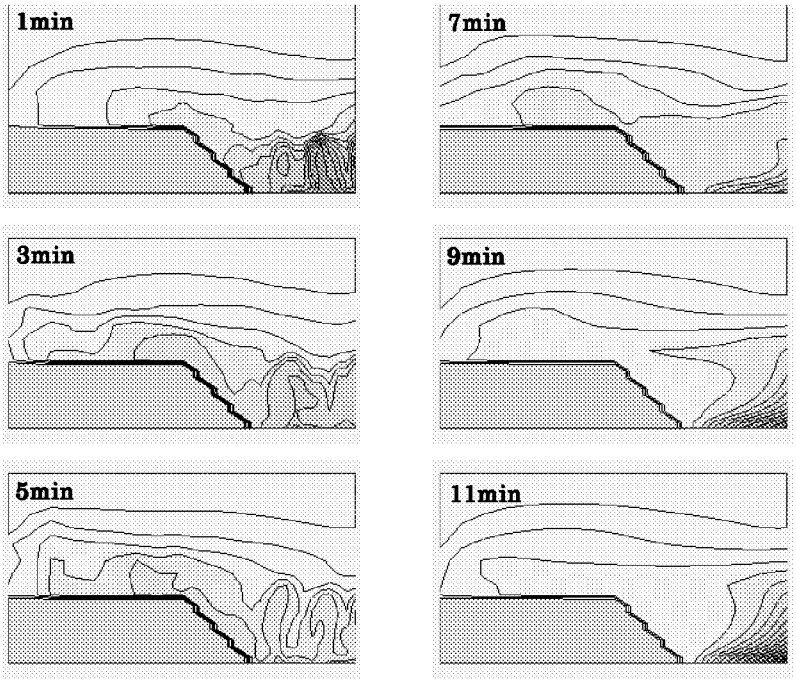

Figure 6: Calculated concentration distributions after 1, 3, 5, 7, 9 and 11min

The main emission sources in Katmandu are vehicle and brick manufacturing [7]. The source of brick manufacturing is assumed to be located at the center of the calculated region and to emit pollutant substance continuously. The diffusion calculation was carried out in these conditions. The calculated concentration distributions of the left side after 1, 3, 5, 7, 9 and 11 min are shown in Fig.6. The pollutant substance is accumulated into the valley from 7 min to 12 min(from sunset to sunrise), since the strong stable layer is formed under the valley. The area of the high concentration emerges at the center of the calculated region. After that, the concentration decreases gradually by the convection.

The typical diurnal variation of NO_x concentration measured in Katmandu on February 2001 is shown in Fig.7. NO_x concentration increases gradually from sunset and has a maximum peak at 6 - 9 a.m. After that, NO_x concentration decreases rapidly by the turbulent mixing. We think that the mainly cause of the increase of NO_x concentration in the midnight is the emission from brick manufacturing and that the cause of the peak concentration is the emission from vehicles. These results showed that the diurnal variation of air pollution concentration in Katmandu valley is strongly influenced by the characteristic climate induced from the geographical feature

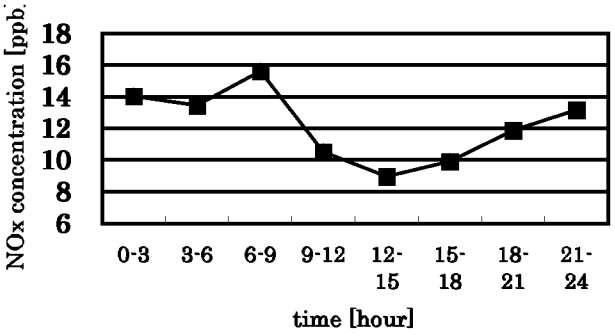

Figure 7: Diurnal variation of NO_x concentration in Katmandu

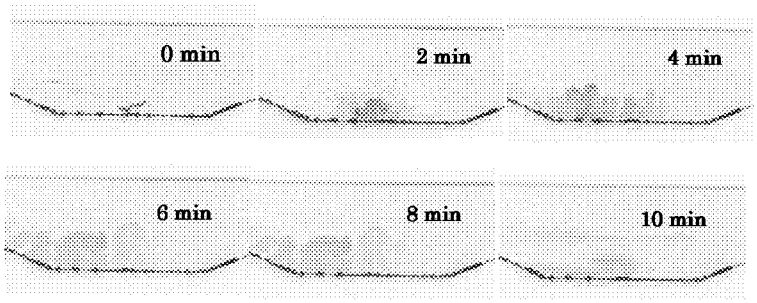

Figure 8: Video images of tracer concentration after 0, 2, 4, 6, 8 and 10min

of Katmandu valley.
At one minutes before the bottom temperature changes to high temperature, tracers were injected into the middle water tank. The decrease of tracers concentration was visualized, and video images were taken. The Video images of tracer concentration after 0, 2, 4, 6, 8 and 10 minute are shown in Fig.8. From Fig.8, the decrease of tracer's concentration by the convection can be seen. These results are basically the same as the variation of the calculated concentration.

5 Conclusion

The mechanism of air pollution in Katmandu valley was simulated by a water tank experiment and by numerical calculation. The updraft wind on the slope and Bénard convection occurred while the bottom temperature was maintained by high temperature. The downdraft wind on the slope occurred and the inversion layer was formed while the bottom temperature was maintained by low temperature. The diffusion calculation was carried

out assuming the emission from brick manufacturing. The variations of calculated concentration were qualitatively agreed with the variations of the observed NO_x concentration in Katmandu valley on February 2001.

References

[1] Shrestha, M. L., Kondo, A., and et.al., Diurnal Variation of Air Pollution Concentration during Winter in Katmandu Valley, *Air Pollution 2002*, **2002**

[2] S. Mitsumoto, Ueda, H. and Ozoe, H., A Laboratory Experiment on the Dynamics of the Land and Sea Breeze, *J. Atmos. Sci.*, 40, 1228-1240 **1983**

[3] Kondo, A., Kaga, A. and et.al., Analysis of Sea and Land Breeze in a Water Tank Experiment and Numerical Simulation and Influence of its Flow Fields on Mass Diffusion, *J.Jpn. Soc. Atmos. Environ.*, 35, 355-367,**2000** (in Japanease)

[4] Kaga, A., Inoue, Y. and Yamaguchi, K., Pattern Tracking Algorithms Using Succesive Abandonment, *J. of Flow Visualization and Image Processing*, 1, 283-296 **1993**

[5] Ueda, H. : Effects of External Parameters on the Flow Field in the Coastal Region – A Linear Model –, *J. Climate and Appl. Meteor.*, 22, 312-321 **1982**

[6] Patankar, S.V. : Numerical Heat Transfer and Fluid Flow, *Hemisphere Publishing Co.* **1980**

[7] The world Bank, Urban air quality management strategy in Asia Kathmandu vally report, **1996**